ISSN 2278-3091
Volume 8, No.1.6, 2019
International Journal of Advanced Trends in Computer Science and Engineering
Available Online at http://www.warse.org/IJATCSE/static/pdf/file/ijatcse7081.62019.pdf
https://doi.org/10.30534/ijatcse/2019/7081.62019

Relativity Drive Transform and Segment Inverse Kinematic for Multi-configuration Rectilinear Gait for Orthogonal Configuration Snake Like Robot

Samsi Md Said[1], Amir Sharizam Ismail[2], Tengku Mohd Azahar Tuan Dir[3], Jamel Othaman[4], Norazlin Ibrahim[5]
Industrial Automation Section, Universiti Kuala Lumpur Malaysia France Institute, 43650 Bandar Baru Bangi Selangor, Malaysia
samsi@unikl.edu.my, amirsharizam@unikl.edu.my, tgazahar@unikl.edu.my, jamel@unikl.edu.my, norazlin@unikl.edu.my

ABSTRACT

Snake like robot is a hyper redundant robot system having very large number of degree of freedom (DOF). Current trend treat the large degree of freedom as a body shape global system. This paper presents Relativity Drive Transform and Segment Inverse Kinematic for Multi-configuration Rectilinear Gait for Orthogonal Configuration Snake like Robot. In this study, large degree of freedom robot system will be decomposed into tail, middle and head group where the number of joints per group will be simplified into two DOF system. Inverse kinematic is being used for the mapping from global body shape world to joint space world. Translational motion in world coordinate can be planned step by step from tail to head using drive transform and its low level joint control value can be derived from inverse kinematic model. Homogeneous transformation and its inversion such as drive transform can be used to model the tail to head locomotion. This drive transform modeling technique can estimate rectilinear gait translational position and speed in Cartesian coordinate world space in comparison to body shape traveling wave locomotion

Key words: Relativity Drive Transform; Segment Inverse Kinematic; Multi-configuration Rectilinear Gait; Orthogonal Configuration Robot.

1. INTRODUCTION

Robotic link and joint can be treated at system level and joint level. System level can be considered high level while at joint space can be considered low level. Low level robot arm focus on controller design. Eduardo I. et all [1] design four DOF pseudo-anthropomorphic robotic arm having shoulder yaw and pitch, elbow pitch and wrist pitch. The motion capture device used is the Microsoft Kinect which detects its operator's arm position. S.V.R.K.Rao et. all [2] develop Brain computer Interface to control portable robot arm.At joint level, A.A.M Zahir et all. [3] used GA to optimize PI controller to regulate speed of cart follower. Robotic arm system can be divided further to mobile and static system. Snake robot can be considered as mobile robotic system. Snake like robot capability to enter narrow space is very useful since narrow space exist either man made (inside aircraft wing or engine), in nature (endoscopy operation for low opening surgery) and disaster areas.

2. LITERATURE REVIEW

Even though the rectilinear gait is more less space consuming in horizontal and vertical direction, most of literature focused type of motion which took large floor area due to serpentine and sidewinding motion most dominant type of locomotion seen in natural snake [3]-[10]. The snake like robot capability to enter narrow space is very useful since narrow space exist either man made (inside aircraft wing or engine), in nature (endoscopy operation for low opening surgery) and disaster areas [11]-[14]. It is estimated that the role of snake like robot as important as today industrial robot for service industry which will capture 7 billion USD worth of market in 2021 [14].

Md. Raisuddin Khan et. al proposed wriggler gait and gait transition from serpentine to wriggler for entering narrow space by considering snake scale but in lateral mode by employing inverse kinematic [20]-[21]. Norzalilah Mohamad Nor and Shugen Ma introduce linear bipolar activation function in Central Pattern Generator (CPG) to control the smooth transition the number of S body shape for serpentine locomotion for entering and adapting to various narrow space width and to avoid external obstacle [22]-[23]. Both works improve the top view serpentine gait by employing Inverse kinematic and CPG for multi configuration snake like robot adapting to narrow space. Several researchers focused on side view locomotion such as rectilinear snake like robot to derive the ability of snake moving into confined space [15]-[19]. The problem of rectilinear gait snake like robot is different mechanical design snake like robots are proposed. There is no uniform design universally used for rectilinear snake like robot. Second, special design using prismatic or sliding joint is employed for rectilinear gait. Prismatic joint is more complex, expensive to build and to maintain in lieu of revolute joint which possess more dexterity and compactness for robotic design method [24]. Third, the sliding prismatic joint creates friction with floor space which causes the need for special anchor points to balance horizontal friction force [25]. In the real field, the coefficient of friction may be very large, and the movement will be stuck which raise the requirement for movement that free from friction or obstacle avoidance movement. Fourth, anchor or pivot points exist that act like stopper to propel rectilinearly the segment of snake robot from tail, middle segment and head. The pivot or anchor point become a major study such as in rectilinear snake like locomotion robot especially in exaggerated linear gait snake like robot that employ variable friction anchor point developed by Hopkins [26]. Three segment rectilinear gaits considering rough surface with dry friction which is scalable into higher degree of freedom robot is introduced by Wenbin Tang and Shugen Ma in [27].

The advantages of employing sliding joints are due to reducing the height signature of snake robot. By using revolute joint the side view profile may be larger and defeat the purpose of employing snake like robot moving into confined space. It is necessary to trade of between unavoidable height profile and friction free forward movement by proposing multi-configuration design using revolute joint that adapt into contour side view profile. To solve problem of too many rectilinear gaits dedicated snake like robot, an orthogonal configuration snake like robot is being proposed in this work. Orthogonal configuration Snake like robot is among the important design since it can perform one plane vertical (rectilinear gait) or horizontal (serpentine) and three-dimensional plane (sidewinding and rolling) [28]-[30]. These measures solve the rectilinear gait friction problem but maintain versatility of orthogonal snake like robot configuration for turning and three-dimension locomotion if needed to bridge to the rectilinear movements. Motoyasu Tanaka and Kazuo Tanaka [31] use orthogonal configuration snake like robot with wheel using pitch axes to control ascending and descending step and using yaw axes for directional control for multi-step rectilinear gait locomotion. Sine wave is being used to generate rectilinear vertical plane locomotion in orthogonal design snake like robot by controlling the amplitude or joint angle and phase angle between adjacent pitch joint [32]. Using sine wave is under approach of traveling waves which creates impact to the ground and body lifting from flat world which cause high torque and energy lost which is unneeded for forward motion. A smooth non-touching linear motion above ground is another potential advantage of relativity drive transform method proposed in this paper.

Orthogonal configuration Snake like robot is among the important design since it can perform one plane vertical or horizontal and three-dimensional plane. In this work we want to focus on simplified arm modeling and screw like Cartesian frame integration to orthogonal design snake like robot. Next, homogeneous transformation and its inversion will be used to describe the relative point configuration between segment or anchor point. A series of homogeneous transformation describing point at tail, middle and head (all refer to global coordinate) will used to describe spatial distance vector between anchor points. Inverse kinematic modular into respective relative two points between one anchor points to another is also proposed in second layer. Next, the Drive transformation will be introduced to govern motion for each sequence of motion from tail, middle and head anchor point or segment. These three-segment motion can be used for infinite or large degree of freedom snake like robot. Introducing relativity drive transform algorithm and using orthogonal design that consists of revolute joints which perpendicularly configured from joint to joint but focusing on the rectilinear gait capability will solve the problems mentioned above. This drive transform modeling technique can estimate rectilinear gait translational position and speed Cartesian coordinate in comparison to body shape traveling wave locomotion

3. METHODOLOGY

Orthogonal configuration snake like robot possess joint axes that are ortho-normal from adjacent joints as in Figure 1. The yaw joint control the top plane movement, while pitch joint control the vertical plane movement. Combination of vertical and horizontal joints can create three-dimensional snake like robot locomotion. Here we focus on odd or pitch joints for creating rectilinear gait but maintain versatility of orthogonal design of snake like robot.

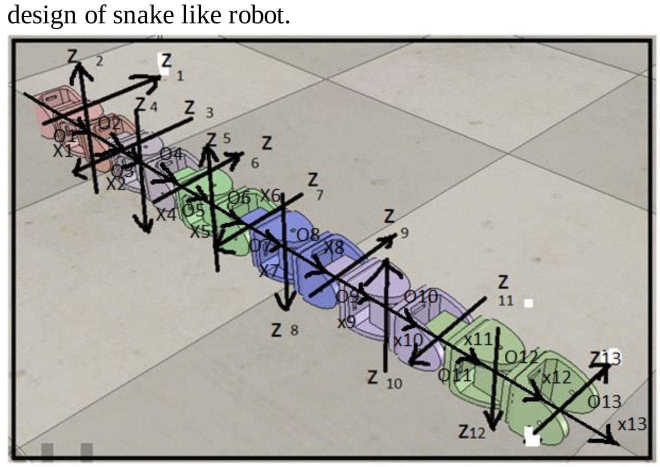

Figure 1: Orthogonal configuration design snake like robot

To enter variable height and multi steps profile contour for both floor and ceiling, multi configuration segment consisting of a series of two pitch joints (odd joints for orthogonal configuration robot) and links will be employed such as displayed in Figure 2. The body shape and speed can be adapted to contour profile (as initial point A configuration) where the bottom joint act as anchor point to ground while the top joint may become constraint points locking to ceiling (as new point B movement configuration) for propelling rectilinearly further the other segment.

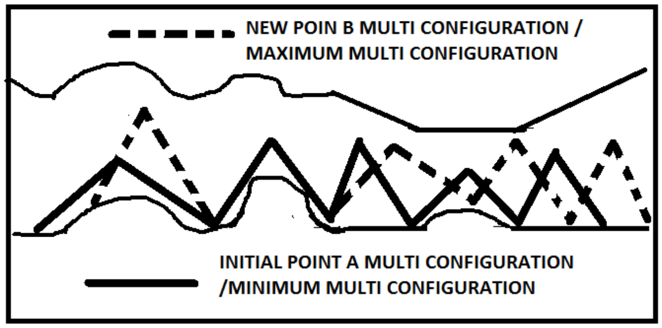

Figure 2: Min-Max Multi configuration adapting to contour floor and ceiling

Relativity Drive Transform and Intra Motion for 3 point Rectilinear Gait using inverse kinematic for Orthogonal Hyper Redundant Robot consists of 3 movement points which is started from point T at the tail, followed by point M at the middle and finally point H at the head. This movement being called relativity since only one point is moving and the other points remain fixing to the ground behaving as pivot. For example, if tail point T moving from point A to point B, the other points as such M and H behave as two pivots which remain at rest or remain at A. Two pivots are needed for stability of one-point movement for three degree or higher degree of freedom system snake like robot. The notation A is for initial point while B is for final point for every point at tail, middle and head section (T, M, H). The nomenclature of TA means tails at beginning point while TB is when tail at the end point. This movement is also called TMH movement according to TMH sequences from point A to B. The sequences of motion are starting from TA to TB, followed by MA to MB and finally HA to HB. Figure 3 shows this motion for tail motion. The gravity and friction of the floor is assumed to be large to lock the static points at rest while allowing the movement sequence displaced without slips at anchoring pivot points.

This algorithm can be used for high degree of freedom snake like robot such as in figure 4 where the tail, head and middle body move simultaneously from point A to B at the first sequence of movement while only middle bodies point move simultaneously at second sequence of pure middle body movement. Note that the pivot and middle body changed alternately from first to second sequence where pivot at first sequence become middle body at second sequence and vice versa. The discussion in this chapter is limited to three degree of freedom TMH movement which stressed important on one by one sequence of movement from tail, middle and head while the intended application is for large degree of freedom snake like robot. In order to apply TMH algorithm for large degree of freedom snake like robot as in figure 4, certain modification need to be done such as simultaneous motion of head, tail and middle body at first sequence and all middle body simultaneous motion at second sequence. Another important consideration here is the opposing nature of inverse kinematic from left and right pair of middle pivots. The challenge is to develop inverse kinematic of opposing nature from left and right segment while maintaining overall structure of forward kinematic from joint 1 to joint N. The inverse kinematic is more important here since it is the product of drive transform that govern the relative motion from point A to point B. Distributed drive transform also major contribution in this work to govern multi relative motion of every points which produce multi configuration large degree of freedom snake like robot system moving in multi-step and variance ceiling height profile contour such as depicted in Figure 2.

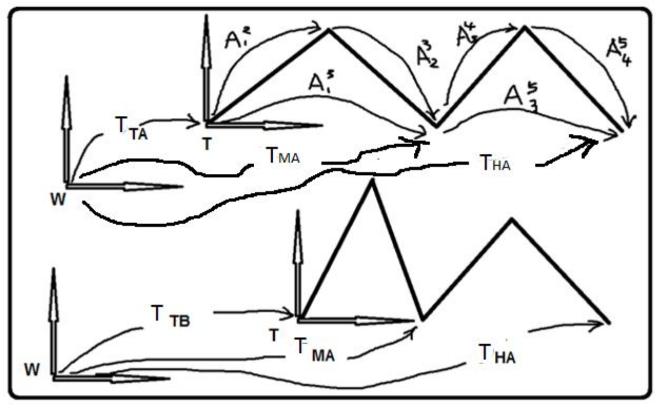

Figure 3: Tail movement from TA to TB

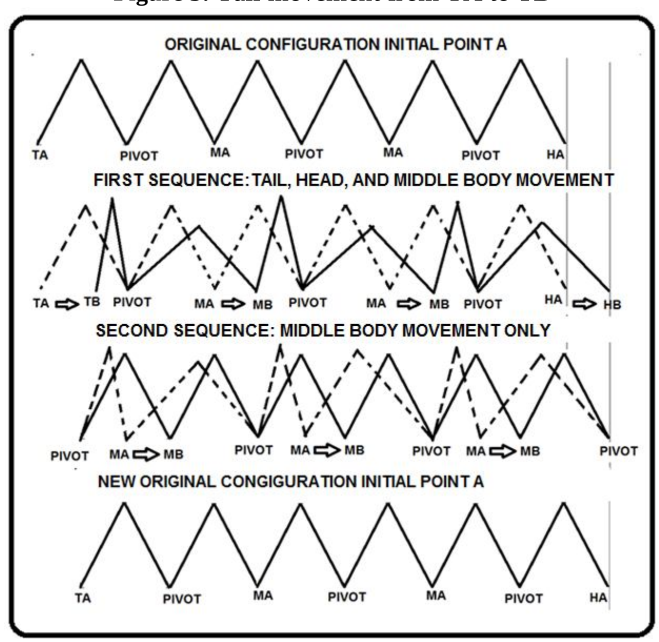

Figure 4: TMH algorithm applied to large degree of freedom snake like robot

In the first layer, homogeneous transformation matrix will be used to describe the robot configuration and the relation between any relative moving points to world coordinate system. By referring to the world both global and local information of any points of interest in snake robot body can be known (combined with forward kinematic of local body frame at each joints). Based on the manipulation of homogeneous transformation the inverse kinematic in second layer will be derived for deciding joint angles to respective robot joint coordinate. Homogeneous transformation is four by four matrix that describe any two Cartesian coordinate frame position and orientation relative to the reference or first frame. The first three rows and three column describe about frame orientation and the fourth column describe the frame vector position and all are based on the first frame. Homogeneous transformation will be used to describe the relative position and orientation between tail and middle points. For finding the left side length parameter from tail to middle point, the middle below configuration as in Figure 5 will be used since we want to maintain the free movement of tail point A and not creating friction with the ground. Refer figure 5 for position of tail T relative to world or T_W^{TA}, position of middle point M relative to the world or T_W^{MA} and position of middle point M relative to the tail T or T_{TA}^{MA}. The notation A is for initial point and B is for displaced new point. Equation (1) describe the relationship and equation (2) and (3) through matrix inversion gives critical parameter between tail to middle point. Utilizing equation (3) the orientation information about rotation about x or θ_X, rotation about y or θ_Y, and rotation about z or θ_Z can be found in equation (4) to (6). The critical length parameter vector between middle to tail point is given in equation (7) and (8) which is extracted from fourth column of equation (3).

$$T_W^{TA} T_{TA}^{MA} = T_W^{MA} \quad (1)$$

$$T_{TA}^{MA} = (T_W^{TA})^{-1} T_W^{MA} \quad (2)$$

$$T_{TA}^{MA} = \begin{bmatrix} n_{xT\_M} & s_{xT\_M} & a_{xT\_M} & P_{xT\_M} \\ n_{yT\_M} & s_{yT\_M} & a_{yT\_M} & P_{yT\_M} \\ n_{zT\_M} & s_{zT\_M} & a_{zT\_M} & P_{zT\_M} \\ 0 & 0 & 0 & 1 \end{bmatrix} \quad (3)$$

$$\theta_X = Atan2\left(\frac{s_{zT_M}}{\sqrt{1-n_{zT_M}^{\;2}}}, \frac{a_{zT_M}}{\sqrt{1-n_{zT_M}^{\;2}}}\right) \quad (4)$$

$$\theta_Y = Atan2\left(-n_{zT\_M}, \sqrt{1-n_{zT\_M}^{\;2}}\right) \quad (5)$$

$$\theta_Z = Atan2\left(\frac{n_{yT_M}}{\sqrt{1-n_{zT_M}^{\;2}}}, \frac{n_{xT_M}}{\sqrt{1-n_{zT_M}^{\;2}}}\right) \quad (6)$$

$$P_T^M = [P_{xT_M} \quad P_{yT_M} \quad P_{zT_M} \quad 1]^T \quad (7)$$

$$L_{1L} = \sqrt{P_{xT_M}^{\;2} + P_{yT_M}^{\;2}} \quad (8)$$

$$L_{2L} = \sqrt{L_{1L}^{\;2} + P_{zT\_M}^{\;2})} \quad (9)$$

For finding the right-side length parameter from middle to head the middle top configuration as in figure 6 will be used since we want to maintain the free movement of middle point M and not creating friction with the ground. Figure 6 describe middle segment point M relative to the world T_W^{MA} and head relative to the world or T_W^{HA} as in equation (10) and (11). Equation (13) extracted the result from vector position information from the fourth column of matrix in equation (12). The critical length parameter vector between middle to head point is given in equation (14) and (15) which is extracted from fourth column of equation (13). Equation (8), (9), (14) and (15) is very important result to control the snake robot left and right segment for subsequent inverse kinematic process in second layer.

$$T_W^{MA} T_{MA}^{HA} = T_W^{HA} \quad (10)$$

$$T_{MA}^{HA} = (T_W^{MA})^{-1} T_W^{HA} \quad (11)$$

$$T_{MA}^{HA} = \begin{bmatrix} n_M^H & s_M^H & a_M^H & P_M^H \\ 0 & 0 & 0 & 1 \end{bmatrix} \quad (12)$$

$$P_{MA}^{HA} = [P_{xM_H} \quad P_{yM_H} \quad P_{zM_H} \quad 1]^T \quad (13)$$

$$L_{2R} = \sqrt{P_{xM\_H}^{\;2} + P_{yM\_H}^{\;2} + P_{zM\_H}^{\;2})} \quad (14)$$

$$L_{1R} = \sqrt{P_{xM\_H}^{\;2} + P_{zM\_H}^{\;2})} \quad (15)$$

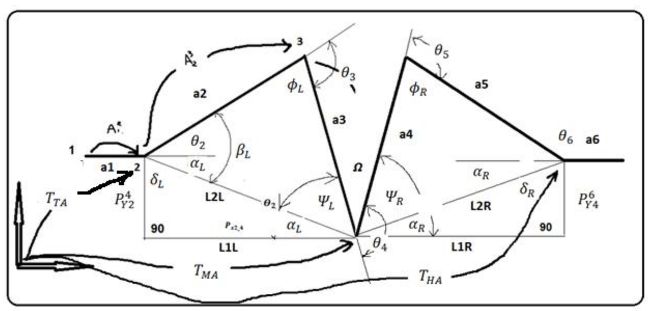

Figure 5: Middle below configuration T_TA, T_MA and T_HA for tail locomotion

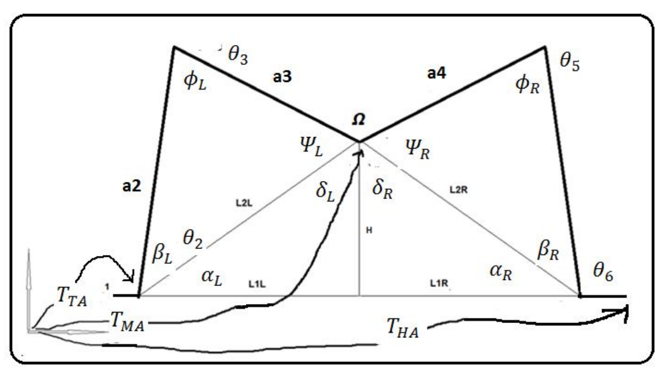

Figure 6: Middle top configuration T_TA, T_MA and T_HA

Drive Transformation from Point A to Point B

Drive transformation will be utilized to describe the contraction and expansion movement of tail, middle and head point from initial point A to new displaced position of point B. The displacement from previous to new point difference is restricted to 60 % in the movement of rectilinear gait in this work as to avoid adjacent link collision since the forward actuation is a byproduct of link-joint angle displacement. The concept of drive transformation for tail is introduced in equation (17) from relation of new position point B from initial point A as described in equation (16). The same approach will be used for middle and head point as developed in equation (19) and (21). Equation (25) to (27) give the new individual vector position from head to tail in vector x, y and Cartesian component for left side while equation (28) to (30) give the same previous information but specified only to right side or head segment. The new corrected length parameter for left segment is given in equation (31) and (32) while for the right segment; the new displaced position is given in (33) and (34).

$$T_{TB} = T_{TA} D(\lambda)_{TA}^{TB} \tag{16}$$

$$D(\lambda)_{TA}^{TB} = (T_{TA})^{-1} T_{TB}) \tag{17}$$

$$T_{MB} = T_{MA} D(\lambda)_{MA}^{MB} \tag{18}$$

$$D(\lambda)_{MA}^{MB} = (T_{MA})^{-1} T_{MB} \tag{19}$$

$$T_{HB} = T_{HA} D(\lambda)_{HA}^{HB} \tag{20}$$

$$D(\lambda)_{HA}^{HB} = (T_{HA})^{-1} T_{HB} \tag{21}$$

$$D(\lambda)_{TA}^{TB} = \begin{bmatrix} n_{TA}^{TB} & s_{TA}^{TB} & a_{TA}^{TB} & P_{TA}^{TB} \\ 0 & 0 & 0 & 1 \end{bmatrix} \tag{22}$$

$$D(\lambda)_{MA}^{MB} = \begin{bmatrix} n_{MA}^{MB} & s_{MA}^{MB} & a_{MA}^{MB} & P_{MA}^{MB} \\ 0 & 0 & 0 & 1 \end{bmatrix} \tag{23}$$

$$D(\lambda)_{HA}^{HB} = \begin{bmatrix} n_{HA}^{HB} & s_{HA}^{HB} & a_{HA}^{HB} & P_{HA}^{HB} \\ 0 & 0 & 0 & 1 \end{bmatrix} \tag{24}$$

$$P_{TA}^{TB} = P_{MA}^{MB} = P_{MA}^{MB} = [P_{dx} \quad P_{dy} \quad P_{dz}]^T$$

$$P_{xT\_MB} = \begin{cases} (P_{xT\_M} - P_{dx}), P_{xT\_B} > P_{xT\_A} \;\&\; P_{xM\_B} = P_{xM\_A} \\ (P_{xT\_M} + P_{dx}), P_{xT\_B} = P_{xT\_A} \;\&\; P_{xM\_B} > P_{xM\_A} \\ (P_{xT\_M}), P_{xT\_B} = P_{xT\_A} \;\&\; P_{xM\_B} = P_{xM\_A} \end{cases} \tag{25}$$

$$P_{yT\_MB} = \begin{cases} (P_{yT_M} + P_{dy}), P_{yT\_B} > P_{yT\_A} \;\&\; P_{yM\_B} = P_{yM\_A} \\ (P_{yT\_M} - P_{dy}), P_{yT\_B} = P_{yT\_A} \;\&\; P_{yM\_B} < P_{yM\_A} \\ (P_{yT\_M}), P_{yT\_B} = P_{yT\_A} \;\&\; P_{yM\_B} = P_{yM\_A} \end{cases} \tag{26}$$

$$P_{zT\_MB} = \begin{cases} (P_{zM\_H} + P_{dz}), P_{zT\_B} > P_{zT\_A} \;\&\; P_{zM\_B} = P_{zM\_A} \\ (P_{zT\_M} - P_{dz}), P_{zT\_B} = P_{zT\_A} \;\&\; P_{zM\_B} < P_{zM\_A} \\ (P_{zT\_M}), P_{zT\_B} = P_{zT\_A} \;\&\; P_{zM\_B} = P_{zM\_A} \end{cases} \tag{27}$$

$$P_{xM\_HB} = \begin{cases} (P_{xM\_H} - P_{dx}), P_{xM\_A} < P_{xM\_B} \;\&\; P_{xH\_A} = P_{xH\_B} \\ (P_{xM\_H} + P_{dx}), P_{xM\_A} = P_{xM\_B} \;\&\; P_{xH\_A} < P_{xH\_B} \\ (P_{xM\_H}), P_{xM\_A} = P_{xM\_B} \;\&\; P_{xT\_A} = P_{xT\_B} \end{cases} \tag{28}$$

$$P_{yM\_HB} = \begin{cases} (P_{yM\_H} - P_{dy}), P_{yM\_A} < P_{yM\_B} \;\&\; P_{yH\_A} = P_{yH\_B} \\ (P_{yM\_H} + P_{dy}), P_{yM\_A} = P_{yM\_B} \;\&\; P_{yH\_A} < P_{yH\_B} \\ (P_{yM\_H}), P_{yM\_A} = P_{yM\_B} \;\&\; P_{yH\_A} = P_{yH\_B} \end{cases} \tag{29}$$

$$P_{zM\_HB} = \begin{cases} (P_{zM\_H} - P_{dz}), P_{zM\_A} < P_{zM\_B} \;\&\; P_{zH\_A} = P_{zH\_B} \\ (P_{zM\_H} + P_{dz}), P_{zM\_A} = P_{zM\_B} \;\&\; P_{zH\_A} < P_{zH\_B} \\ (P_{zM\_H}), P_{zM\_A} = P_{zM\_B} \;\&\; P_{zH\_A} = P_{zH\_B} \end{cases} \tag{30}$$

$$L_{1LB} = \sqrt{P_{xT\_MB}^{\;2} + P_{yT\_MB}^{\;2}} \tag{31}$$

$$L_{2LB} = \sqrt{L_{1L}^{\;2} + P_{zT\_MB}^{\;2})} \tag{32}$$

$$L_{1RB} = \sqrt{P_{xM\_HB}^{\;2} + P_{yM\_HB}^{\;2}} \tag{33}$$

$$L_{2RB} = \sqrt{L_{1RB}^{\;2} + P_{zM\_HB}^{\;2})} \tag{34}$$

Segment Inverse Kinematic

To map from left and right segment homogeneous drive transformation result from point A to point B for implementing tail, intra motion of middle segment M and head point, inverse kinematic operation is needed in layer 2. The and right and left segment inverse kinematic is build using cosine rule and trigonometric relation as displayed from equation (35) to (54). Equation (55) to (60) give the joint space coordinate value for joint 1 till joint 6 (odd joint for orthogonal robot such as joint 1,3,5 and 7) for tail and head movement. Equation (62) to (67) give the joint space coordinate result for middle segment configuration and intra movement.

$$\alpha_L = Atan2\left(\frac{P_{y2\_4}}{L_{1L}}, \frac{L_{1L}}{L_{2L}}\right) \tag{35}$$

$$\alpha_R = Atan2\left(\frac{P_{y4\_6}}{L_{1R}}, \frac{L_{1R}}{L_{2R}}\right) \tag{36}$$

$$\alpha_{LB} = Atan2\left(\frac{P_{y2\_4B}}{L_{1LB}}, \frac{L_{1LB}}{L_{2LB}}\right) \tag{37}$$

$$\alpha_{RB} = Atan2\left(\frac{P_{y4\_6B}}{L_{1RB}}, \frac{L_{1RB}}{L_{2RB}}\right) \tag{38}$$

$$\delta_L = 90 - \alpha_L \quad (39)$$

$$\delta_R = 90 - \alpha_R \quad (40)$$

$$\delta_{LB} = 90 - \alpha_{LB} \quad (41)$$

$$\delta_{RB} = 90 - \alpha_{RB} \quad (42)$$

$$\beta_L = Atan2\left(\sqrt{1-\left[\frac{a_2^2+L_{2L}^2-a_3^2}{2a_2L_{2L}}\right]^2}, \frac{a_2^2+L_{2L}^2-a_3^2}{2a_2L_{2L}}\right) \quad (43)$$

$$\beta_R = Atan2\left(\sqrt{1-\left[\frac{a_5^2+L_{2R}^2-a_4^2}{2a_5L_{2R}}\right]^2}, \frac{a_5^2+L_{2R}^2-a_4^2}{2a_5L_{2R}}\right) \quad (44)$$

$$\beta_{LB} = Atan2\left(\sqrt{1-\left[\frac{a_2^2+L_{2LB}^2-a_3^2}{2a_2L_{2LB}}\right]^2}, \frac{a_2^2+L_{2LB}^2-a_3^2}{2a_2L_{2LB}}\right) \quad (45)$$

$$\beta_{RB} = Atan2\left(\sqrt{1-\left[\frac{a_5^2+L_{2RB}^2-a_4^2}{2a_5L_{2RB}}\right]^2}, \frac{a_5^2+L_{2RB}^2-a_4^2}{2a_5L_{2RB}}\right) \quad (46)$$

$$\phi_L = Atan2\left(\sqrt{1-\left[\frac{a_2^2-L_{2L}^2+a_3^2}{2a_2L_{2L}}\right]^2}, \frac{a_2^2-L_{2L}^2+a_3^2}{2a_2L_{2L}}\right) \quad (47)$$

$$\phi_R = Atan2\left(\sqrt{1-\left[\frac{a_4^2-L_{2R}^2+a_5^2}{2a_4L_{2R}}\right]^2}, \frac{a_4^2-L_{2R}^2+a_5^2}{2a_4L_{2R}}\right) \quad (48)$$

$$\phi_{LB} = Atan2\left(\sqrt{1-\left[\frac{a_2^2-L_{2LB}^2+a_3^2}{2a_2L_{2LB}}\right]^2}, \frac{a_2^2-L_{2L}^2+a_3^2}{2a_2L_{2LB}}\right) \quad (49)$$

$$\phi_{RB} = Atan2\left(\sqrt{1-\left[\frac{a_4^2-L_{2RB}^2+a_5^2}{2a_4L_{2RB}}\right]^2}, \frac{a_4^2-L_{2RB}^2+a_5^2}{2a_4L_{2RB}}\right) \quad (50)$$

$$\Psi_L = Atan2\left(\sqrt{1-\left[\frac{a_4^2-a_5^2+L_{2L}^2}{2a_4L_{2L}}\right]^2}, \frac{a_4^2-a_5^2+L_{2L}^2}{2a_4L_{2L}}\right) \quad (51)$$

$$\Psi_R = Atan2\left(\sqrt{1-\left[\frac{a_4^2-a_5^2+L_{2R}^2}{2a_4L_{2R}}\right]^2}, \frac{a_4^2-a_5^2+L_{2R}^2}{2a_4L_{2R}}\right) \quad (52)$$

$$\Psi_{LB} = Atan2\left(\sqrt{1-\left[\frac{a_4^2-a_5^2+L_{2LB}^2}{2a_4L_{2LB}}\right]^2}, \frac{a_4^2-a_5^2+L_{2LB}^2}{2a_4L_{2LB}}\right) \quad (53)$$

$$\Psi_{RB} = Atan2\left(\sqrt{1-\left[\frac{a_4^2-a_5^2+L_{2RB}^2}{2a_4L_{2RB}}\right]^2}, \frac{a_4^2-a_5^2+L_{2RB}^2}{2a_4L_{2RB}}\right) \quad (54)$$

$$\theta_{1t} = 0 \quad (55)$$

$$\theta_{2t} = \beta_L + \alpha_L \quad (56)$$

$$\theta_{3t} = 180 - \phi_L \quad (57)$$

$$\theta_{4t} = (\Psi_R + \Psi_L + \delta_R + \delta_L) - 180 \quad (58)$$

$$\theta_{5t} = 180 - \phi_R \quad (59)$$

$$\theta_{6t} = \beta_R + \alpha_R \quad (60)$$

$$\Omega = 360 - (\Psi_R + \Psi_L + \delta_R + \delta_L) \quad (61)$$

$$\theta_{1b} = 0 \quad (62)$$

$$\theta_{2b} = \beta_L - \alpha_L \quad (63)$$

$$\theta_{3b} = 180 - \phi_L \quad (64)$$

$$\theta_{4b} = \theta_{TM} = \Psi_R + \Psi_L + \alpha_R + \alpha_L \quad (65)$$

$$\theta_{TM} = -(\Psi_L + \alpha_L) \quad (66)$$

$$\theta_{5b} = 180 - \phi_R \quad (67)$$

4. RESULTS AND DISCUSSION

The Relativity Drive Transform algorithm developed previously has been implemented using Scilab program for multiple configurations at left and right segment of orthogonal configuration design snake like robot as in figure 7. Notice the rectangular block horizontal orientation for odd link joint related to orthogonal snake like robot. For simulation purpose the arm length is equal to 1000mm (in real life would be much smaller value) and notice the odd joints of 1, 3, 5 and 7 which define the vertical side view are being manipulated in every sequences (the result of figure 8 angle 1=joint1, angle 2=joint3, angle 3=joint5, angle 4=joint7 for orthogonal configuration). The special forward kinematic for arm modeling will be discussed in future work in order to maintain the focus scope of this paper. Refer figure 7 for multi configuration of tail equal to 0.3 and head equal value to 0.7 for rectilinear motion from tail, middle and head Section which is ideal for entering hole or converging motion. Total displacement is governed by tail movement which is 720 mm as in first row and fourth column matrix of DT_WTAB in figure 8. Figure 8 shows the numerical value of transformation in the first layer and the joint angle result needed for joint space actuation in lower second inverse kinematic layer. Figure 9 show the configuration of tail equal 0.7 and head equal to 0.3 which is in reverse from figure 8 which is intended for exiting from hole or diverging configuration locomotion. Total displacement is governed by tail movement which is 1680 mm as in first row and fourth column matrix of DT_WHAB in figure 8 since the tail is similar to head configuration of 0.7 value as in figure 7. Figure 10 show multi configuration of tail and head both equal value to 1 for rectilinear motion from tail, middle and Head Section which is ideal for movement in constant ceiling hole such is in pipe or aircraft wing. Total displacement is governed by tail movement which is 2400 mm as in first row and fourth column matrix of DT_WTAB in figure 11. Figure 11 shows the numerical value of transformation in the first layer and the joint angle result needed for joint space actuation in inverse kinematic second layer.

It seems that entering confined space configuration is the lowest displacement and speed drive transform which equal to 720mm and exiting hole is higher which equal 1680mm per unit time. The movement with configuration 1 for both tail and head segment gave the highest displacement per unit time which is equal to 2400mm.

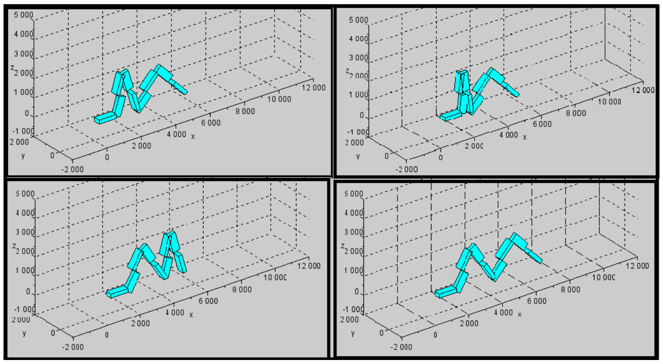

Figure 7: Configuration (Tail=0.3, Head =0.7) Rectilinear motion from tail, middle and Head Section

```
   2.

k

   1.    0.    0.    0.
   0.    1.    0.    0.
   0.    0.    1.    0.
   0.    0.    0.    1.

T_WTA

   1.    0.    0.    720.
   0.    1.    0.    0.
   0.    0.    1.    0.
   0.    0.    0.    1.

T_WTB

   1.    0.    0.    720.
   0.    1.    0.    0.
   0.    0.    1.    0.
   0.    0.    0.    1.

DT_WTAB

   480.         83.107897
L1LA         angle1
   480.         166.21579
L2LA         angle2
   2800.        128.68089
L1RA         angle3
   2800.        91.145992
 L2RA        angle4
```

```
   3.

k

   1.    0.    0.    2200.
   0.    1.    0.    0.
   0.    0.    1.    0.
   0.    0.    0.    1.

T_WMA

   1.    0.    0.    3880.
   0.    1.    0.    0.
   0.    0.    1.    0.
   0.    0.    0.    1.

T_WMB

   1.    0.    0.    1680.
   0.    1.    0.    0.
   0.    0.    1.    0.
   0.    0.    0.    1.

 DT_WMAB

   2160.        57.316361
L1LA         angle1
   2160.        114.63272
L2LA         angle2
   1120.        131.05616
L1RA         angle3
   1120.        147.47959
 L2RA        angle4
```

```
   4.

k

   1.    0.    0.    5000.
   0.    1.    0.    0.
   0.    0.    1.    0.
   0.    0.    0.    1.

T_WHA

   1.    0.    0.    6680.
   0.    1.    0.    0.
   0.    0.    1.    0.
   0.    0.    0.    1.

T_WHB

   1.    0.    0.    1680.
   0.    1.    0.    0.
   0.    0.    1.    0.
   0.    0.    0.    1.

 DT_WHAB

   2160.        57.316361
L1LA         angle1
   2160.        114.63272
L2LA         angle2
   2800.        102.88936
L1RA         angle3
   2800.        91.145992
 L2RA        angle4
```

Figure 8: Result for configuration (Tail=0.3, Head =0.7) for tail, middle and Head Section

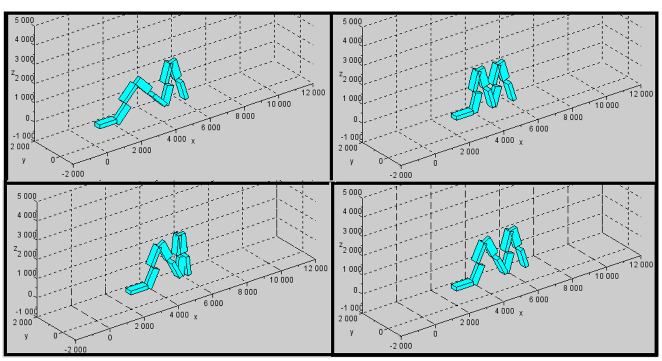

Figure 9: Configuration (Tail=0.7, Head =0.3) Rectilinear motion from tail, middle and Head Section

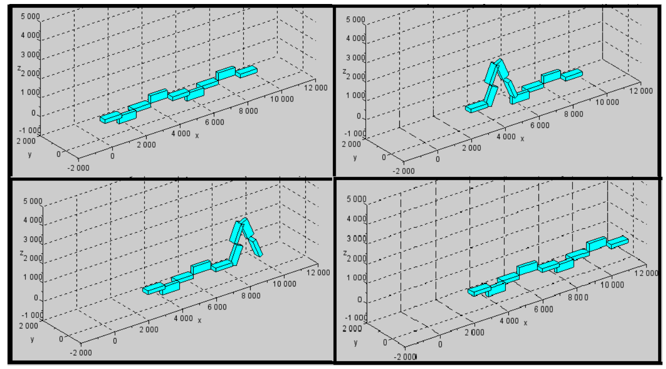

Figure 10: Configuration(Tail=1,Head =1) Rectilinear motion from tail, middle and Head Section

```
   2.

k

   1.    0.    0.    0.
   0.    1.    0.    0.
   0.    0.    1.    0.
   0.    0.    0.    1.

T_WTA

   1.    0.    0.    2400.
   0.    1.    0.    0.
   0.    0.    1.    0.
   0.    0.    0.    1.

T_WTB

   1.    0.    0.    2400.
   0.    1.    0.    0.
   0.    0.    1.    0.
   0.    0.    0.    1.

DT_WTAB

   1600.        66.421822
L1LA         angle1
   1600.        132.84364
L2LA         angle2
   4000.        66.421822
L1RA         angle3
   4000.        0.
 L2RA        angle4
```

```
   3.

k

   1.    0.    0.    5000.
   0.    1.    0.    0.
   0.    0.    1.    0.
   0.    0.    0.    1.

T_WMA

   1.    0.    0.    7400.
   0.    1.    0.    0.
   0.    0.    1.    0.
   0.    0.    0.    1.

T_WMB

   1.    0.    0.    2400.
   0.    1.    0.    0.
   0.    0.    1.    0.
   0.    0.    0.    1.

 DT_WMAB

   4000.        0.
L1LA         angle1
   4000.        0.
L2LA         angle2
   1600.        66.421822
L1RA         angle3
   1600.        132.84364
 L2RA        angle4
```

```
   4.

k

   1.    0.    0.    9000.
   0.    1.    0.    0.
   0.    0.    1.    0.
   0.    0.    0.    1.

T_WHA

   1.    0.    0.    11400.
   0.    1.    0.    0.
   0.    0.    1.    0.
   0.    0.    0.    1.

T_WHB

   1.    0.    0.    2400.
   0.    1.    0.    0.
   0.    0.    1.    0.
   0.    0.    0.    1.

 DT_WHAB

   4000.        0.
L1LA         angle1
   4000.        0.
L2LA         angle2
   4000.        0.
L1RA         angle3
   4000.        0.
 L2RA        angle4
```

Figure 11: Result for configuration (Tail=1,Head =1) for tail, middle and Head Section

5. CONCLUSION

The objectives of the study have been achieved. The TMH Relativity drive transform successfully programmed in Scilab to model the movement and multi configuration of snake like robot. Figure 9 clearly shows body shape longer in tail successfully perform progressive TMH motion involving two DOF system one movement at a time. Figure 10 clearly shows body shape fair distribution of body shape between tail and head able to move progressive TMH motion involving two joints system segmented time movement. Configuration equal to one show highest elevation profile viewed from side plane and this body shape ratio is suitable for entering high opening hole. This shows that the maximum potential is configuration equal to one since it have more room for link lifting from horizontal surface if the ceiling do not pose a height constraint. The need for multiple configurations other than 1 is for variable shape hole as in figure2 where Min-Max

Multi configuration adapting to contour floor and ceiling is needed. Next, the multiple configurations also can optimize the shape of the robot adapting to contour height profile so that the best speed can be achieved. The hole contour floor also have different coefficient of friction and not flat as in the lab environment which need snake like robot of multiple configuration capability to search the best anchoring place for tail, middle and head point (to use obstacle as forward aided motion).

REFERENCES

[1]. Eduardo I. Cabral Jr., Christopher Lambert M. Flores, Geromin S. Nepomuceno III, Jesus Lorenzo A. Singson and Gerald P. Arada, Kinect-based Teleoperated Pseudo-Anthropomorphic Robotic Arm International Journal of Advanced Trends in Computer Science and Engineering, Vol.8 No 5, September - October 2019, pp.2240 – 2245.
https://doi.org/10.30534/ijatcse/2019/59852019

[2]. S.V.R.K.Rao, M Kaivalya, Ch Janaki Devi, M V N Raju, Enhancing those BCI interface execution on aggravate brain-controlled portable robots, International Journal of Advanced Trends in Computer Science and Engineering, Volume 7, No.6, November - December 2018, pp 159-162.
https://doi.org/10.30534/ijatcse/2018/20762018

[3]. Z. Zimmermann, I. Zeidis, C. Behn, Mechanics of Terrestrial Locomotion with a Focus on Nonpedal Motion Systems, Springer, Heidelberg;1992.

[4]. J. Steigenberger and C. Behn, Gait generation considering dynamicsfor artificial segmented worms, ROBOTICS AND AUTONOMOUS SYSTEMS., vol. 59, 2011, pp 555-562.

[5]. S.Hirose. Biologically Inspired Robots:Snake like locomotors and manipulators,Oxford University Press,Oxford 1993.

[6]. S.Ma Analysis of snake movement forms for realization of snake like robot .on proceeding IEEE international Conference Robotics and Automation,Detroit MI USA Volume 4. May 1999,pp3007-3013.

[7]. Ryo Ariizumi and Fumitoshi Matsuno,Dynamical Analysis of Sidewinding Locomotion by a snake like Robot on proceeding IEEE international Conference Robotics and Automation,Karlsruhe Germany May 2013,pp5149-5154.

[8]. Zhelong, WangQin, GaoHongyu Zhao. CPG-Inspired Locomotion Control for a Snake Robot Basing on Nonlinear Oscillators.Journal of Intelligent & Robotic Systems.February 2017, Volume 85, Issue 2, pp 209–227.

[9]. Chaohui Gong, Ross L. Hatton and Howie Choset Conical Sidewinding 2012 IEEE International Conference on Robotics and Automation RiverCentre, Saint Paul, Minnesota, USA May 14-18, 2012.
https://doi.org/10.1109/ICRA.2012.6225377

[10]. Chaohui Gong, Matthew J. Travers, Xiaozhou Fu and Howie Choset, Extended Gait Equation for Sidewinding 2013 IEEE International Conference on Robotics and Automation (ICRA) Karlsruhe, Germany, May 6-10, 2013.

[11]. J.K. Hopkins, B.W. Spranklin, S.K. Gupta, A Survey of Snake-Inspired Robot Designs, Bioinspiration Biomimetics., vol. 4(2), 2009, p 021001.

[12]. A.A. Transeth, K.Y. Pettersen, P. Liljeback, A Survey on Snake Robot Modeling and Locomotion, Robotica., vol. 27, 1950, pp 999-1015.

[13]. A. R. McNeill, Principles of Animal Locomotion. Princeton University Press, 2003.7540

[14]. Snake Robots Market Shares, Strategies, and Forecasts, Worldwide,2015 to 2021, WinterGreen Research INC.2015.

[15]. H. Marvi, J. Bridges, and D. L. Hu, “Snakes mimic earthworms: propulsion using rectilinear travelling waves.” Journal of the Royal Society, Interface / the Royal Society, vol. 10, no. 84, p. 20130188, 2013.

[16]. M. Tesch, K. Lipkin, I. Brown, R. Hatton, A. Peck, and a. H. C.J. Rembisz, “Parameterized and scripted gaits for modular snake robots,” Advanced Robotics, vol. 23, no. 9, pp. 1131–1158, 2009.

[17]. L. I. van Griethuijsen and B. A. Trimmer, “Kinematics of horizontal and vertical caterpillar crawling,” The Journal of Experimental Biology, vol. 212, pp. 1455–62, 2009
https://doi.org/10.1242/jeb.025783

[18]. A.H. Chang, M.M. Serrano, and P.A. Vela, Shape-Centric Modeling of Traveling Wave Rectilinear Locomotion for Snake-Like Robots2016 IEEE 55th Conference on Decision and Control (CDC) ARIA Resort & Casino December 12-14, 2016, Las Vegas, USA.

[19]. Wenbin Tang, Fabian Reyes and Shugen Ma Study on Rectilinear Locomotion Based on a Snake Robot with Passive Anchor2015 IEEE/RSJ International Conference on Intelligent Robots and Systems (IROS) Congress Center Hamburg Sept 28 - Oct 2, 2015. Hamburg, Germany 67 – 3809 TA TEHNICA CORVINIENSIS – Bulletin of Engineering.

[20]. Raisuddin Khan, M. Watanabe and A.A. Shafie Kinematics Model of Snake Robot Considering Snake Scale– American Journal of Applied Sciences 7 (5): 669-674, 2010 ISSN 1546-9239 © 2010Science Publications.

[21]. Md. Raisuddin Khan, Mad Helmi Ab Majid, Shahrul Na’im Sidek, “A Snake Robot with Mixed Gaits Capability,” The 4th KKU International Engineering Conference 2012 (KKU-IENC 2012) .

[22]. Norzalilah Mohamad Nor and Shugen Ma, Body Shape Control of a Snake-like Robot Based on Phase Oscillator Network, Proceeding of the IEEE International Conference on Robotics and Biomimetics (ROBIO) Shenzhen, China, December 2013.
https://doi.org/10.1109/ROBIO.2013.6739471

[23]. Norzalilah Mohamad Nor and Shugen Ma, CPG-based Locomotion Control of a Snake-like Robot for Obstacle Avoidance, 2014 IEEE International Conference on Robotics & Automation (ICRA) Hong Kong Convention and Exhibition Center May 31 - June 7, 2014. Hong Kong, China.

[24]. Zoran Pandilov and Vladimir Dukovski Comparison Of The Characteristics Between Serial And Parallel Robots Acta Tehnica Corviniensis – Bulletin of Engineering Tome VII [2014] Fascicule 1 [January – March] ISSN: 2067 – 3809 AC e VII [2014] Fascicule 1 [January – March]ISSN: 2067 – 3809.

[25]. Hopkins, J. K. and Gupta, S. K., 2012, "Characterization of Forward Rectilinear-Gait Performance for a Snake-Inspired Robot," In the Proceedings of the 2012 Performance Metrics for Intelligent Systems (PerMIS'12) Workshop, College Park, MD.

[26]. J.K. Hopkins, and S.K. Gupta, Design and Modeling of a New Drive System and Exaggerated ectilinear-Gait for a Snake-Inspired Robot,J. Mechanisms Robotics., vol. 6(2), 2014, pp 1138-1146.

[27]. Wenbin Tang and Shugen Ma Analysis of Rectilinear Motion of a Three-Segment Snake Robot Under Action of Dry Friction 2015 IEEE International Conference on Robotics and Automation (ICRA) Washington State Convention Center Seattle, Washington, May 26-30, 2015.

[28]. Juan Gonzalez-Gomez,, Houxiang Zhang,, Eduardo Boemo1 and Jianwei Zhang,Locomotion Capabilities of a Modular Robot with Eight Pitch-Yaw-Connecting Modules.www.iearobotics.com.

[29]. Wright, C., Buchan, A., Brown, B., Geist, J., Schwerin, M., Rollinson, D., Tesch, M. and Choset, H., 2012, "Design and Architecture of the Unified Modular Snake Robot," In the 15th Proceedings of the 2012 IEEE International Conference on Robotics and Automation (ICRA), Saint Paul, MN.

[30]. Li Chena, Shugen Mab, Yuechao Wangb, Bin Lib, Dengping Duana .Design and modelling of a snake robot in traveling wave locomotion.Mechanism and Machine Theory.Volume 42, Issue 12, December 2007, Pages 1632–1642.

[31]. Motoyasu Tanaka and Kazuo Tanaka Control of a Snake Robot for Ascending and Descending Steps, IEEE TRANSACTIONS ON ROBOTICS, VOL. 31, NO. 2, APRIL 2015
https://doi.org/10.1109/TRO.2015.2400655

[32]. Florian Enner, David Rollinson and Howie Choset Simplified Motion Modeling for Snake Robots Robotics and Automation (ICRA), 2012 IEEE International Conference on, 4216-4221.
https://doi.org/10.1109/ICRA.2012.6225163